IJMMM International Journal of Minerals, Metallurgy and Materials 矿物冶金与材料学报（英文版）

Characterization of local chemical ordering and deformation behavior in high entropy alloys by transmission electron microscopy

Qiuhong Liu, Qing Du, Xiaobin Zhang, Yuan Wu, Andrey A. Rempel, Xiangyang Peng, Xiongjun Liu, Hui Wang, Wenli Song, and Zhaoping Lü

Cite this article as:
Qiuhong Liu, Qing Du, Xiaobin Zhang, Yuan Wu, Andrey A. Rempel, Xiangyang Peng, Xiongjun Liu, Hui Wang, Wenli Song, and Zhaoping Lü, Characterization of local chemical ordering and deformation behavior in high entropy alloys by transmission electron microscopy, *Int. J. Miner. Metall. Mater.*, 31(2024), No. 5, pp. 877-886. https://doi.org/10.1007/s12613-024-2884-x

View the article online at SpringerLink or IJMMM Webpage.

INTERNATIONAL JOURNAL OF
Minerals, Metallurgy and Materials

Volume 31, Number 5, May 2024
Page 877

Invited Review https://doi.org/10.1007/s12613-024-2884-x

Characterization of local chemical ordering and deformation behavior in high entropy alloys by transmission electron microscopy

Qiuhong Liu[1),*], *Qing Du*[2),*], *Xiaobin Zhang*[1),✉], *Yuan Wu*[1)], *Andrey A. Rempel*[3)], *Xiangyang Peng*[4)], *Xiongjun Liu*[1)], *Hui Wang*[1)], *Wenli Song*[5,6)], *and Zhaoping Lü*[1),✉]

1) Beijing Advanced Innovation Center for Materials Genome Engineering, State Key Laboratory for Advanced Metals and Materials, University of Science and Technology Beijing, Beijing 100083, China
2) School of Materials Science and Engineering, Ocean University of China, Qingdao 266100, China
3) Institute of Metallurgy of the Ural Branch of the Russian Academy of Sciences, Ekaterinburg 620016, Russia
4) China Nuclear Power Technology Research Institute Co. Ltd., Shenzhen 518000, China
5) Institute of High Energy Physics, Chinese Academy of Sciences (CAS), Beijing 100049, China
6) Spallation Neutron Source Science Center, Dongguan 523803, China
(Received: 4 March 2024; revised: 14 March 2024; accepted: 18 March 2024)

Abstract: Short-range ordering (SRO) is one of the most important structural features of high entropy alloys (HEAs). However, the chemical and structural analyses of SROs are very difficult due to their small size, complexed compositions, and varied locations. Transmission electron microscopy (TEM) as well as its aberration correction techniques are powerful for characterizing SROs in these compositionally complex alloys. In this short communication, we summarized recent progresses regarding characterization of SROs using TEM in the field of HEAs. By using advanced TEM techniques, not only the existence of SROs was confirmed, but also the effect of SROs on the deformation mechanism was clarified. Moreover, the perspective related to application of TEM techniques in HEAs are also discussed.

Keywords: high entropy alloys; transmission electron microscopy; short-range ordering; deformation mechanisms

1. Introduction

Metallic materials have played an important role in promoting the development of human society. For conventional alloys, such as aluminum alloys and steels, their properties were mainly improved through alloying strategies, but they are increasingly unable to meet the needs of modern industrial development. High entropy alloys (HEAs) constitute a new alloy design concept, which brings the possibility of developing new high-performance metallic materials [1]. Nowadays, HEAs and their structural and mechanical properties have attracted extensive attention from scientists [2–4]. In early studies, HEAs were generally considered as random solid solutions with randomly distributed constituent atoms at lattice sites [5–6]. However, recent studies have shown that short-range orderings (SROs) are formed during solidification or/and heat treatment due to the complex elemental environment and interactions between adjacent atoms [7–9]. Controlling the formation of SROs is considered as a promising way for improving the performance of HEAs. Nevertheless, characterizing SROs in multi-component alloys and establishing the relationship between SROs and performance improvement remains a challenge.

Transmission electron microscopy (TEM) and its scanning mode are powerful tools for finely characterizing material structures at the small length scale. Mechanical response induced by SROs have been illustrated by TEM observations in some binary systems such as Ni–Cr and Cu–Mn alloys [10–11]. With the development of aberration correction techniques, atomic-scale characterization has become more and more precise. Especially, high angle annular dark field (HAADF) and annular bright field (ABF) scanning transmission electron microscopy (STEM) combined with spherical aberration correctors, energy dispersive X-ray spectroscopy (EDS) with large silicon drift detectors (SDD) are widely used in identifying the SRO structures. Moreover, recently developed imaging techniques such as integrated differential phase contrast (iDPC) and four-dimensional scanning transmission electron microscopy (4D-STEM) have elevated the microstructural and chemical characterizations of SROs to new heights. As an interdisciplinary field between physics and material science, TEM and its various imaging techniques provide new approaches and ideas for in-depth study of SROs in HEAs.

[*] These authors contributed equally to this work.
✉ Corresponding authors: Xiaobin Zhang E-mail: zhangxb@ustb.edu.cn; Zhaoping Lü E-mail: luzp@ustb.edu.cn

In this short communication, we review the latest progresses in characterizing SROs using different TEM techniques, including high-resolution TEM (HRTEM) with atomic resolution EDS, energy-filtered TEM (EFTEM), HAADF/ABF-STEM, iDPC-STEM, and so on. These are effective ways for revealing the structure, composition, and atomic packing of local chemical structures in HEAs at the atomic scale [12]. Moreover, effects of SROs on the deformation mechanism based on TEM observations are also discussed. Future research areas about application of TEM in decoding the local chemical structures in HEAs are elaborated sequentially. We aim to provide not only the research front about SROs in HEAs but also thought-provoking ideas to inspire future studies.

2. Characterizing SRO by TEM

In some binary alloys, SROs were identified as the existence of an ordered arrangement of atomic pairs, which could consist of different atoms over a range of several atomic scales. Despite the complex interatomic interactions between multiple components in HEAs, an increasing number of studies have shown that the atomic arrangement out of the ideal disorder in HEAs would lead to the formation of SROs, such as atomic clusters [13], nanodomains and superlattices [14], and ordered interstitial complexes [15]. The existence of SROs in HEAs has been demonstrated through computational simulations [16–17]. However, it is still challenging to precisely characterize SROs through experiments, which are mainly due to their small size, complexed compositions, varied locations, and so on. Several ways have been tried to characterize the existence of SROs. Guo *et al.* [18] studied the distorted local structure of $Zr_{1/3}Nb_{1/3}Hf_{1/3}$ alloy through neutron and X-ray scattering. Maiti and Steurer [8] studied the clusters enriched in Hf and Zr in the single-phase TaNbHfZr through atom probe tomography (APT). However, there are obvious limitations to the above approaches. High-energy X-ray results show the overall scattering rather than the local information of site occupation. APT results have the problems like atomic loss and atomic displacement during the collection of excited atoms. Therefore, more accurate and direct characterizing technique of SROs is necessary to understand their effects on the mechanical properties of HEAs.

With the development of aberration-correction techniques in (S)TEM, atom-by-atom characterization is no longer a problem for most materials. Especially for STEM, it has several kinds of imaging modes (like bright field, ABF, and HAADF) with distinct advantages. HAADF-STEM images are easy to interpret and benefit in characterizing the presence of heavy elements, because the image contrast is proportional to the atomic number. While ABF-STEM is suitable for characterizing the presence of light elements due to cutting off of direct electron beam. The existence of SROs can be revealed by combing HAADF and ABF images. Lei *et al.* [15] doped TiZrHfNb HEAs with 2at% O, and obtained substantially improved tensile strength and ductility, which broke the strength–ductility trade-off. They then identified the Zr/Ti-rich and Hf/Nb-rich regions in the TiZrHfNb alloy through aberration-corrected STEM at HAADF mode, and directly observed the oxygen atoms in ordered oxygen complexes (OOCs) at ABF mode. Oxygen atoms were supposed to locate in the octahedral or tetrahedral interstitials of body-centered cubic (bcc) structure (Fig. 1(a)–(c)). To exactly determine the occupying sites of oxygen atoms, Jiao *et al.* [19] further explored the formation of OOCs in the oxygen-doped bcc TiZrNb medium entropy alloy (MEA) by combining the HAADF-STEM images with integral differential phase contrast (iDPC) STEM images. Different from HAADF, iDPC-STEM has the advantage of low-dose and high signal-to noise (S/N) ratio [20–21], which is specially benefit in detecting the interstitial atoms against a black background [22–23]. As shown in Fig. 1(d)–(h), light element (Ti, Zr) enrichment regions and heavy element (Nb) enrichment regions can be clearly identified in oxygen-doped TiZrNb MEA. O atomic columns were identified as weak contrast nearby the Ti/Zr atoms, which indicates the formation of local ordering structures of OOCs. Up to now, two strategies, microalloying and heat treatment have been applied to control the formation of SROs in the HEAs. Atomic-resolved EDS has the advantage of revealing the differences in chemical affinity between elements and can be applied to analyze the distribution of elements in SROs formed by microalloying. Ding *et al.* [24] replaced Mn with Pd in conventional Cantor alloys (CrMnFeCoNi), and found through EDS analysis that the distribution of all elements changed, rather than simply replacing Mn with Pd. Meanwhile, there was no obvious aggregation preference for elements, indicating that lattice distortion in HEAs enhanced the driving force for the formation of SROs, as shown in Fig. 2(a).

Heat treatment is another strategy for regulating SROs. For example, annealing has been adopted in HEAs to change the atoms distribution from absolutely disordered to locally ordered. These locally ordered structures result in the superlattice spots in the selected area electron diffraction patterns (SAEDP) and the bright regions in the dark field image. As reported by Dasar *et al.* [25], SAEDP and HRTEM results showed that CoFeNi MEA containing Al (9.1at%) and Ti (5.7at%) had a strong tendency to form $L1_2$ domain after annealing at 500°C for 0.5 h. Furthermore, the HAADF-STEM images provide more structural information of SROs. Wang *et al.* [26] reported that in the annealed $Ti_{50}Zr_{18}Nb_{15}V_{12}Al_5$ HEAs, the surface spacing of the B2 structure SRO was twice that of the substrate (Fig. 2(b)). Chen *et al.* [27] also found SRO regions with similar characteristics in annealed VCoNi MEA through HAADF-STEM. Filtered images which has better S/N ratio reflected the V/Co(Ni)/V staggered structure (Fig. 2(c)).

Recently, several advanced techniques such as adaptive propagation ptychography (APP) have been developed to accurately detect atomic occupancy. APP can be used to detect light element atoms in the metal matrix, which is based on the

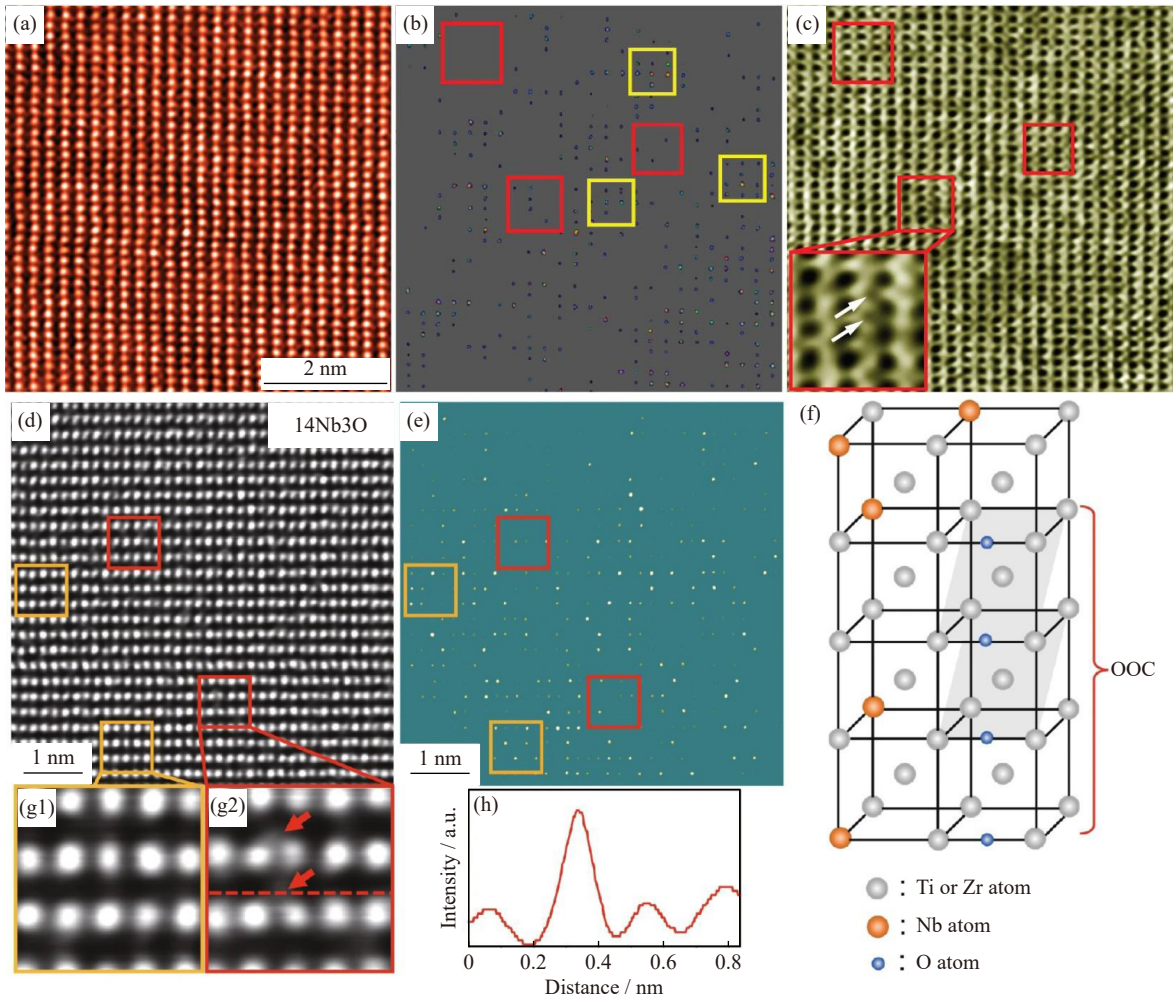

Fig. 1. Chemical characterizations of ordered oxygen complexes in the $(TiZrHfNb)_{98}O_2$ HEA [15] and $TiZr_{30}Nb_{14}O_3$ MEA [19]: (a) HAADF-STEM image for the [011] bcc crystal axis of $(TiZrHfNb)_{98}O_2$ HEA; (b) contrast analysis of (a) revealing the distribution of OOCs (red squares represent the Zr/Ti-rich regions, and yellow squares indicate the Hf/Nb-rich regions); (c) ABF-STEM image of the same region as (a) (inset is an enlarged view of the OOC, with the white arrows indicating the positions of the oxygen atomic columns); (d, e) the iDPC images for the [011] bcc crystal axis with contrast analysis to reveal the existence of chemical short-range orderings in the $TiZr_{30}Nb_{14}O_3$ MEA (red squares represent the Ti/Zr-rich regions, and orange squares indicate the Nb-rich regions); (g1, g2) the enlargements of the orange and red squares in (d), revealing the formed OOCs; (f) schematic diagram of the OOC; (h) intensity line profile of the red dashed line in (g2), which is obtained by the standard tool of Digital Microscopy software. (a–c) Reprinted by permission from Springer Nature: *Nature*, Enhanced strength and ductility in a high-entropy alloy via ordered oxygen complexes, Z.F. Lei, X.J. Liu, Y. Wu, *et al.*, Copyright 2018.

phase liner imaging principle [28–29]. In comparison with the HAADF, ABF, and iDPC imaging techniques, APP has the advantage of ultra-high resolution at the sub-Å level and imaging of the light and heavy atoms simultaneously. Moreover, APP is particularly suitable for observing alloys with large lattice distortions, such as M/HEAs. Liu *et al.* [30] directly observed the specific occupancy of oxygen atoms in bcc $(TiNbZr)_{86}O_{12}C_1N_1$ MEAs with a high concentration of oxygen atoms for the first time using the APP technique (Fig. 3(a) and (b)). Layered imaging along the [110] and [111] axes combined with three-dimensional (3D) views of the crystal structure determined that the oxygen atoms in $(TiNbZr)_{86}O_{12}C_1N_1$ occupied not only the octahedral interstitial position (O), but also the tetrahedral interstitial position (T), which is different from conventional MEAs containing interstitial atoms. Moreover, the number of oxygen atoms located in the T and the O sites confirms the possibility of the hypothesis that high concentration of interstitial atoms can adjust the lattice occupation. In addition, electron tomography (ET) in TEM 3D reconstruction technology has attracted much attention in materials analysis. By taking projections of the sample in different directions and combining with the FFT patterns, the direct 3D spatial configuration of the sample can be obtained, so that the 3D structure such as crystal orientation, dislocations, and defects can be observed. This efficient and high-resolution method breaks down the barrier of only obtaining two-dimensional images (Fig. 3(c)). Using ET technology, not only the local structural features such as SROs in M/HEAs [31], but also the short and medium range order of 3D atomic arrangements in metallic glasses [32] have been successfully obtained.

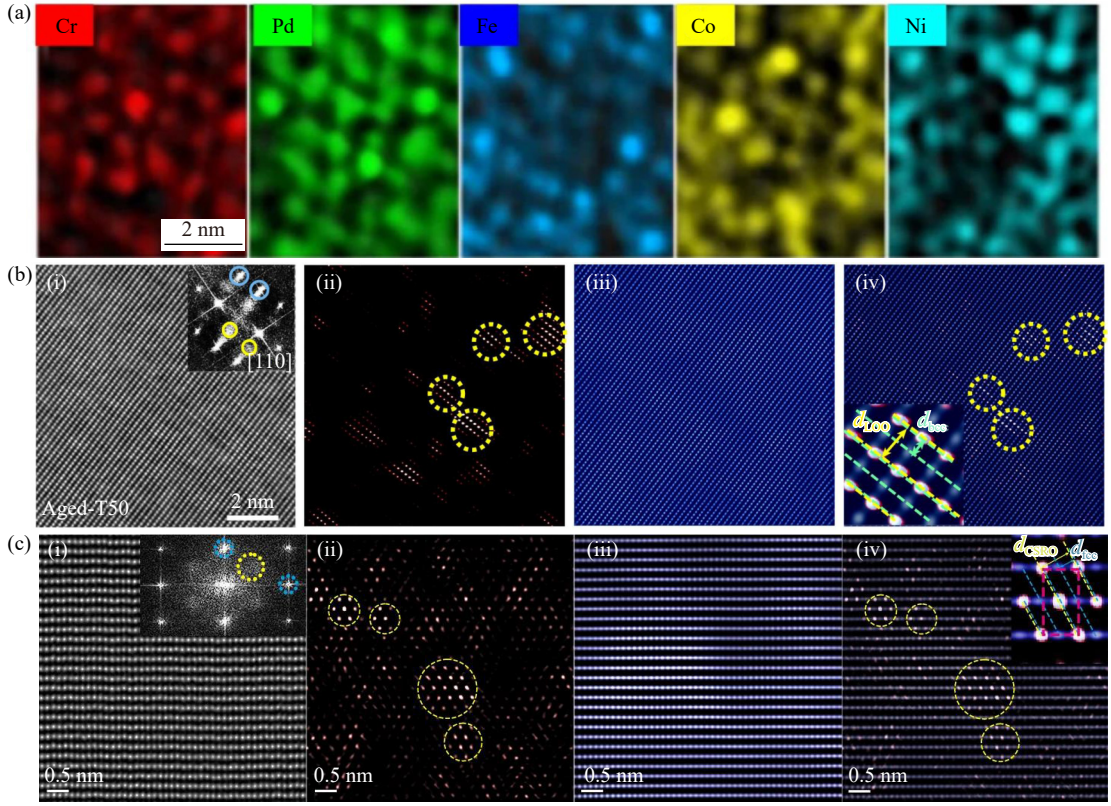

Fig. 2. Typical characterization of the short-range ordering in HEAs: (a) EDS mapping of the local concentration distribution of individual elements in the same region in face-centered cubic structure (fcc) CrPdFeCoNi HEA [24]; (b) the atomic structure morphology of the aged $Ti_{50}Zr_{18}Nb_{15}V_{12}Al_5$ HEAs reflected from (i) the HAADF-STEM lattice images and the corresponding fast Fourier transform (FFT) patterns (inset), with yellow solid circles marking the extra discs due to the SROs and blue solid circles marking the Braggs spots of bcc matrix, (ii) the IFFT images obtained from the extra discs, with yellow circles marking the several representative SRO regions, (iii) the IFFT images obtained from the bcc Braggs spots, showing the bcc lattice, and (iv) the images superimposing corresponding SROs and bcc IFFT images (d_{bcc} is the spacing of {001} planes in the normal bcc lattice, while d_{LCO} is the spacing corresponding to the extra LCO) [26]; (c) evidence of chemical short-range order (CSRO) in fcc VCoNi MEA, including (i) the lattice image of the fcc phase with extra diffraction spots in the corresponding FFT patterns (insert), (ii, iii) the IFFT image showing the CSRO regions (several are circled) and the fcc lattice, respectively, and (iv) the superimposed image of (ii) and (iii), with a close-up view of a CSRO region in the inset (d_{fcc} denotes the spacing of $\{\bar{3}11\}$ planes in the normal fcc lattice, whereas d_{CSRO} displays the spacing corresponding to the extra chemical order) [27]. (a) Reprinted by permission from Springer Nature: *Nature*, Tuning element distribution, structure and properties by composition in high-entropy alloys, Q.Q. Ding, Y. Zhang, X. Chen, *et al*., Copyright 2019. (b) Reprinted by permission from Springer Nature: *Nat. Mater.*, Tailoring planar slip to achieve pure metal-like ductility in body-centred-cubic multi-principal element alloys, L. Wang, J. Ding, S.S. Chen, *et al*., Copyright 2023. (c) Reprinted by permission from Springer Nature: *Nature*, Direct observation of chemical short-range order in a medium-entropy alloy, X.F. Chen, Q. Wang, Z.Y. Cheng, *et al*., Copyright 2021.

3. Revealing plastic deformation carriers in HEAs by TEM

In conventional alloys, the traditional solid solution strengthening theory is commonly used to explain the effect of alloying on the deformation mechanism, owing to the similar atomic environment in the matrix and the significant difference between solute and solvent elements. Additionally, second-phase strengthening [33–34], grain boundary strengthening [35–36], and dislocation strengthening [37–38] have been successfully induced in conventional alloys to achieve simultaneous improvement in both strength and plasticity. In contrast to conventional alloys, the deformation behavior of HEAs shows some unique features as the result of the high entropy effects, like local chemical ordering [39] and lattice distortion [40]. Zhao *et al.* [41] showed that the deformation mode of the typical Cantor alloy FeCoNiCrMn varies with the increase of strain rate, including dislocation, twinning, strain, or stress induced phase transformation, and even formation of amorphous phase.

TEM plays an important role in identifying the different deformation mechanisms. Direct observation of the morphology of dislocations can be conducted through advanced TEM based on the theory of strain-lining imaging. Dislocations in the HEAs bring local lattice distortions which leads to the bending of the atomic plane. Due to the distortion of the local lattice at Bragg angle, electron diffraction deviated from the central electron beam, making it possible to image the dislocation from a different diffraction plane. With the accumulation of deformation, different dislocation movements

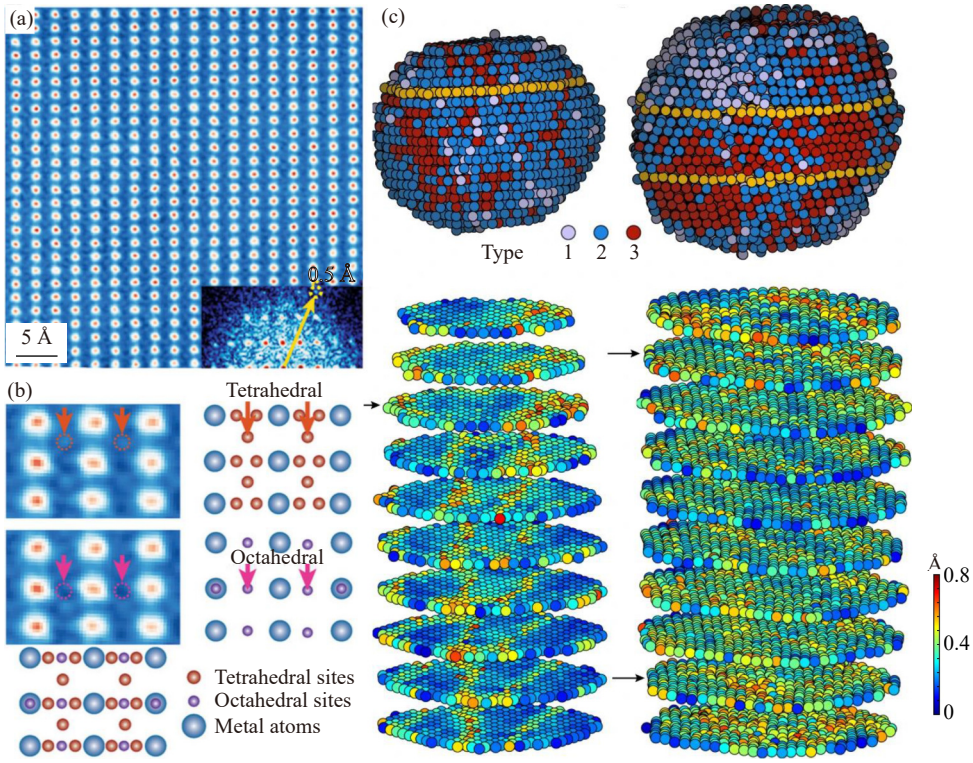

Fig. 3. Investigation of the atomic site occupation in HEAs: (a) observation of the O-12 alloy along the [110] zone axis (inset shows the corresponding FFT pattern, indicating a spatial resolution of 0.5 Å) and (b) close-up image of (a), compared with structural models of bcc lattice containing T-site and O-site interstitials projected along the [110] zone axis. The oxygen interstitials occupy the T-sites, rather than the O-sites, in this region [30]; (c) experimental atomic models of two HEAs and atomic layer-by-layer visualization of the 3D displacement [31]. (a, b) C. Liu, J.Z. Cui, Z.Y. Cheng, *et al.*, *Adv. Mater.*, vol. 35, art. No. e2209941 (2023) [30]. Copyright Wiley-VCH Verlag GmbH & Co. KGaA. Reproduced with permission. (c) Reprinted by permission from Springer Nature: *Nature*, Three-dimensional atomic structure and local chemical order of medium- and high-entropy nanoalloys, S. Moniri, Y. Yang, J. Ding, *et al.*, Copyright 2023.

from slip to entanglement and plugging occur. Both dislocation–dislocation interactions and further dislocation generated from the lattice distortions contributes to the work hardening of HEAs. Therefore, it is critical to understand the dislocation enhancement mechanism by the direct observation of the detailed dislocation behavior in HEAs. Xiong *et al.* [42] identified the movement type of dislocations in the matrix and B2 phases in two-phase eutectic HEA $AlCoCrFeNi_{2.1}$ using double-beam diffraction TEM imaging. The TEM bright-field images directly show the origin of the plasticity and strength. On the one hand, the slip transfer of the dislocations at the interface promotes synergistic deformation of the two phases. On the other hand, the strong hindering effect of the interface on the dislocations effectively improved the strength. Zhang *et al.* [43] also observed the rapid movement of Shockley dislocations and the formation of corresponding stacking faults at the crack tip during the early stages of CrMnFeCoNi deformation through the *in-situ* strain analysis in TEM.

Although strength can be significantly improved through the dislocation strengthening mechanism, loss of plasticity remains a challenge to overcome. Other defects in the deformation process of HEAs, such as stacking fault, twinning, and even amorphous phases have also been studied. Liu *et al.* [44] accurately measured the stacking fault energy (SFE) of several typical fcc HEAs through dark-field TEM and demonstrated that the reduction of SFEs contributes to the formation of more deformation twins. Moreover, reducing SFE can effectively increase the width of dislocation extension, thus inhibiting cross-slip transition of dislocation to twin. The twins are characterized based on the specific diffraction spots between the twin and matrix in the diffraction pattern, combined with the obvious brightening bands in the dark field image, as shown by Deng *et al.* [45] and Jiang *et al.* [46]. Laplanche *et al.* [47] observed the twins in the NiCoCr alloys and investigated the extended dislocation width, confirming that twins were responsible for the high yield strength and work-hardening rate at low strain levels. With the development of *in-situ* TEM, real-time observation and simultaneous high-resolution imaging have greatly enriched the experimental conditions and techniques. Recently, Wang *et al.* [48] directly observed the dynamic deformation process of the crack tips of ultrafine cantor alloys from crystalline to amorphous using *in-situ* technique. By comparing the morphology changes throughout the crystal-amorphous transformation using HRTEM, it was concluded that the transformation was triggered by both the high lattice friction and the high grain boundary resistance to dislocation slip at small grain sizes resulted high-stress accumulation at the crack tip.

4. Effects of SROs on deformation mechanism revealed by TEM

In conventional alloys such as Cu–Al alloy [49], the SRO caused by the addition of solute elements has a significant influence on the deformation behavior. The *in-situ* TEM techniques help to clarify the interplay between SFE and SRO, and the resultant deformation process of submicron-sized Cu–Al single-crystalline pillars. As discussed above, the complex atomic environment in the HEAs not only promotes the formation of SROs but also changes SFE by regulating SROs, hence affecting deformation modes including dislocation slip, deformation twinning, and phase transformation, and thereby bringing the new understanding of the deformation mechanism of HEAs.

4.1. Effect of SROs on dislocation nucleation and slip

In contrast to the direct atomic exchange with vacancies in conventional alloys with single-principal element, the vacancy migration process in multi-principal component entropy alloys is a joint behavior of different atoms, resulting in higher activation energy for dislocation nucleation [50]. Moreover, the non-random occupation of SRO atoms implies chemical fluctuations, which further affects the dislocation nucleation through the migration process. Smith *et al.* [51] analyzed Frank-Read dislocation sources in refractory HEAs using a phase-field dislocation kinetic model and found that the existence of SROs reduced the mean critical activation stress of the Frank-Read sources. Zhao *et al.* [52] demonstrated that the extent of chemical short-range ordering in FeCrCoNiMn HEAs can be improved via high temperature aging, which means the overall strengthening of the alloy can be reflected by increasing the stress required for homogeneous dislocation nucleation.

Although it's difficult to study the dislocation nucleation by TEM, it is still quite useful to explore the influence of SROs on the slip behavior of the HEAs to understand the deformation mechanism. On one hand, the SROs can overcome the energy barriers brought by the "diffuse antiphase boundary" and accordingly create channels for dislocation slip. As the dislocation motion in Cu–Mn alloys [53] and Ni–Cr alloys [54], leading dislocations in HEAs disrupt the ordered regions as they pass through the SROs, resulting in a reduction in local lattice resistance. Subsequently, the dislocations are inclined to slip in plane due to the reduced resistance. As shown in Fig. 4, Bu *et al.* [55] conducted dynamic observation of the interaction process between SROs and dislocations in HfNbTiZr bcc HEA with the help of *in-situ* strain experiments. TEM images show that with the increase of local stress, the dislocations gradually experienced the process of slipping, local pinning, and finally detaching from the pinning to form a dislocation ring. Moreover, through the combination of STEM and APT, it is determined that the pinning points are Hf-rich and Nb-rich clusters, which not only leads to the mismatch of atomic radii, but also leads to fluctuations in local lattice strain. Furthermore, SROs cause frequent dislocation pinning and local double cross-slip, which together promote the plasticity enhancement of HfNbTiZr bcc HEA. Additionally, the SROs also induce a "slip surface softening effect" [56], whereby dislocations in the HEAs are easily captured by energetically favorable regions and repelled by negative ones, forming wavy dislocation lines. Lei *et al.* [15] reported that the addition of oxygen atoms to O-2 HEA promotes cross-slip, and the plastic deformation mechanism changes from planar to "wavy" slip via *in-situ* strain experiments. Chen *et al.* [27] also observed the wavy path of dislocations through the SROs region in VCoNi MEAs. In other words, the deformation behavior of fcc HEAs involves multiple cooperative mechanisms of edge and screw dislocations [57]. He *et al.* [58] also observed that there are many stacking faults at the interface between the SROs and the austenitic matrix near the fracture of FeMnCoCrN HEAs, suggesting that the existence of SROs also has a hindering effect on the dislocation movement during the plastic deformation.

4.2. Effect of SROs on stacking fault

The deformation mode of HEAs is also controlled by SFE, which has a significant effect on the dislocation mobility, cross-slip capacity, deformation twinning, and even phase transformations [59]. In contrast to conventional alloys, the local compositional diversity in the multi-principal component alloy tends to bring differences in SFE. Owing to the SROs, shearing displacements on the stacking faults result in changes in both the order of the atoms and the ordered state in the region of the stacking faults, which finally leads to the increase of SFE. Ding *et al.* [60] calculated by density functional theory that the average SFE of CrCoNi alloys changes with the increase of SROs. While the SFE can be obtained through measuring the width of the extended dislocations in a TEM image [44]. Zhang *et al.* [61] showed that the SFE ($(23.33 \pm 4.31)\ mJ\cdot m^{-2}$) of the CrCoNi alloys with locally ordered structures was twice that of the alloy without aging ($(8.18 \pm 1.43)\ mJ\cdot m^{-2}$) (Fig. 5). Further experiments confirmed the effects of SROs on SFE.

On the other hand, the increased SFE could inhibit the movement of dislocations, resulting in the accumulation of dislocations and cross-slip phenomenon. For example, Ding *et al.* [24] performed *in-situ* deformation experiments on CrFeCoNiPd alloys, and the results showed that the presence of SROs during plastic deformation at room temperature transformed the original two $\frac{1}{6}\langle 112\rangle\{111\}$ partial dislocations to a 60° full dislocation. It is revealed by the variations in the width of the dislocation cores that the locally ordered structure could cause fluctuations in the width of the stacking fault, i.e., increasing the SFE. As confirmed by Lei *et al.* [15], promoted cross-slip of dislocations and enhanced dislocation interactions can be demonstrated by *in-situ* TEM and HAADF, indicating the hardening and strengthened toughness.

Furthermore, SROs can affect twinning and phase transformation through the stacking faults [60], which is mainly

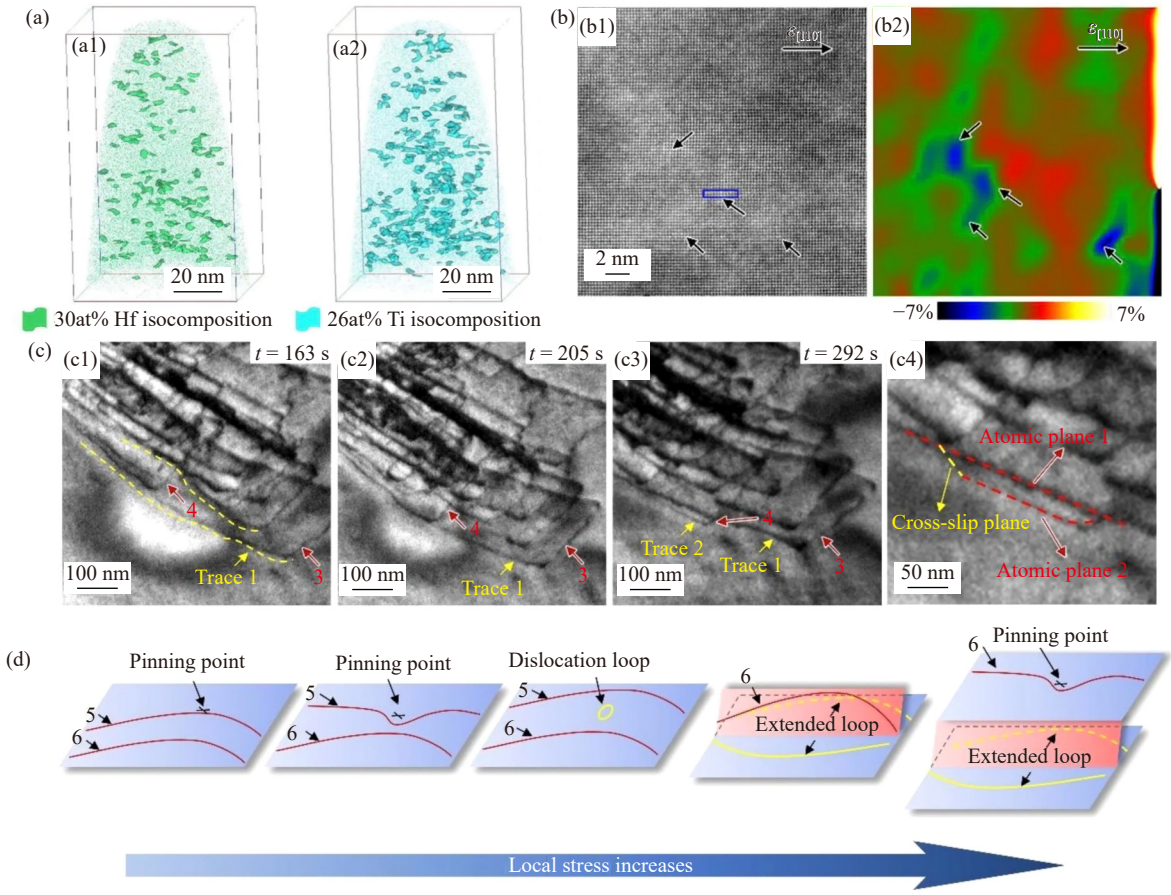

Fig. 4. SRO induced dislocation pinning, multiplication, and cross slip in HfNbTiZr bcc HEA [55]: (a) atom probe tomography 3D reconstructions of an as-cast sample with the threshold for the iso-composition surface of (a1) 30at% Hf and (a2) 26at% Ti, which highlights the Hf-rich and Ti-rich clusters; (b1) atomic resolution HAADF–STEM image of a pinned dislocation and (b2) geometric phase analysis (GPA) of the same region ($\varepsilon_{[110]}$ represents the local strain of (110) interplanar spacing); (c) local double cross-slip induced spatial distribution of planar slips and the concomitant pinning induced multiplications (c1–c4); (d) the schematic illustrates that the pinning assisted by cross-slips enhances the dislocations multiplication and makes the planar slips and dislocation multiplication incidents spatially distribute. Reprinted from *Mater. Today*, 46, Y.Q. Bu, Y. Wu, Z.F. Lei, *et al*, Local chemical fluctuation mediated ductility in body-centered-cubic high-entropy alloys, 28-34, Copyright 2021, with permission from Elsevier.

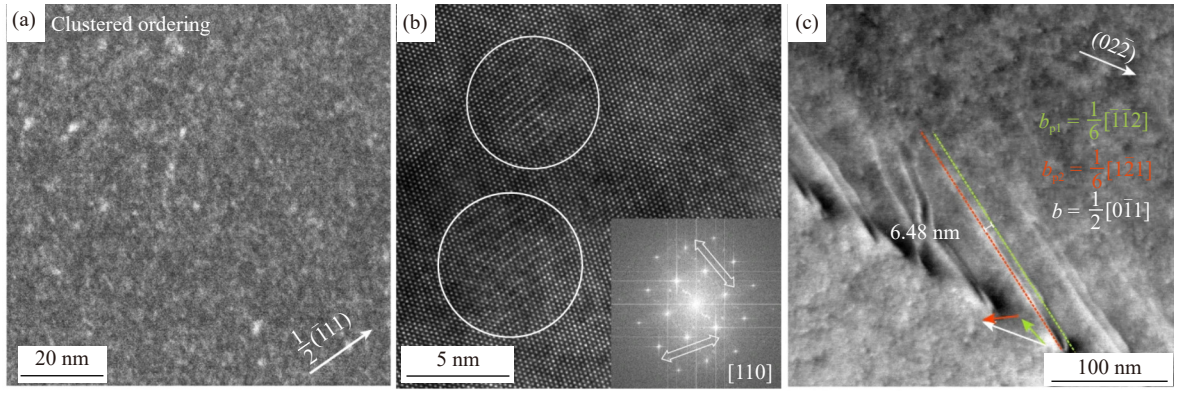

Fig. 5. (a) Dark-field images and (b) the associated high-resolution TEM images of the SROs in the 1000°C aged CrCoNi MEA (inset in (b) is the associated FFT image); (c) low angle annular dark field (LAADF) images showing dislocation dissociations [61] (b_{p1} and b_{p2} are two different 1/6⟨112⟩{111} partial dislocations, and b represents a 60° full dislocation). Reprinted by permission from Springer Nature: *Nature*, Short-range order and its impact on the CrCoNi medium-entropy alloy, R.P. Zhang, S.T. Zhao, J. Ding, *et al*., Copyright 2020.

based on the range of transformation pressure in HEAs. It was found that HEAs containing SROs exhibit higher critical pressures of fcc–hexagonal close packed (hcp) transformation. Therefore, the locally ordered structures promote the accumulation of dislocations and the interaction between dislocations and hcp phases [62].

5. Perspective

TEM has exhibited great advantages in identifying SROs in HEAs. However, it is a fact that the specific atomic structure of SROs remains complex. It is undeniable that future work is needed to establish a quantitative relationship between SROs and the mechanical properties. In our view, the following aspects of TEM need to be urgently addressed.

5.1. Structural description of SROs

As described above, ABF, HAADF, and *in-situ* TEM have already played a key role in identifying the SROs in HEAs. However, visualization of details including the 3D atomic arrangement or the exact elemental distribution still cannot be realized precisely. The development of the atomic reconstruction techniques including 3D-APT and ET enabled acquiring the configurations in nanoscale. The characterization of SRO requires more direct evidence by TEM techniques, in addition to the identification of superlattice reflections. Walsh *et al.* [63] believed that the existence of the superlattice reflections should not be regarded as incontrovertible evidence for SROs, because of the absence of additional expected peaks. For example, in the characterization of CuPt type ordered structures, there should theoretically be rows of atomic columns in the Cu element rich and depleted regions on the $(1\bar{1}1)$. Nevertheless, the associated diffraction peaks are missing in all experimental representations, both from electron diffraction and the FFT patterns of the dark field image. Another theory is that smaller, less resolvable nanoscale surface defects and surface steps will also form a similar diffraction phenomenon. Altogether, larger-sized data of atomic configuration with reliable SROs is necessary for the deeper study of structure, performance and computational simulation.

5.2. Structure–property relationship mediated by SROs

Although the simultaneous increase in strength and plasticity has been successfully realized through regulating the SROs in the matrix, it is still confusing for establishing the quantitative structure–property relationship. Meanwhile, the effect of SROs on the formation and evolution of different crystal defects requires detailed investigation. *In-situ* TEM with different environment currently allows real-time observation for the evolution of the deformed microstructure, fulfilling the in-depth applications in the fields of physics, chemistry, materials, and biology. Ultimately, these will contribute to controlling the performance of HEAs through regulating the SROs.

5.3. Effect of electron irradiation on SROs

In order to meet the demand of high-resolution imaging, high-energy electron beam leads to the strong interaction between the high-energy electron and the atoms in the sample. There does exist the microstructure transformation induced by the electron irradiation in the previous study [64–66]. Considering the challenge in understanding the evolution of SROs, electron irradiation provides not only a new route but also a precise location for the sample to study the SROs. Moreover, the multifunctional TEM enables the experiments with different temperatures and environmental conditions.

6. Summary

Short-range ordered structures have been demonstrated to exist in chemically long-range disordered HEAs as a common phenomenon. The formation of SROs in M/HEAs can be controlled by composition design and heat treatment process. Although the existence of SROs has been largely demonstrated by the simulation, it is still challenging to experimentally characterize them due to their small size, complexed compositions, and varied locations.

The development of advanced TEM techniques provides the possibility to systematically study the local structures of HEAs (usually SROs). In addition, observing the structure of SROs with TEM and corresponding interaction with dislocations and stacking faults are benefit to the in-depth understanding of the formation of SROs and its effect on the performance of HEAs. Obviously, integration of different TEM techniques and other means for the characterization of local structure are urgently needed to facilitate the developments in both atomic physics and materials science.

Acknowledgements

This study was financially supported by the National Natural Science Foundation of China (Nos. 51971017, 52271003, 52071024, 52001184, and 52101188), the National Science Fund for distinguished Young Scholars, China (No. 52225103), the Funds for Creative Research Groups of China (No. 51921001), the National Key Research and Development Program of China (No. 2022YFB4602101), the Projects of International Cooperation and Exchanges NSFC (No. 52061135207), and the Fundamental Research Funds for the Central Universities, China (No. FRF-TP-22-130A1).

Conflict of Interest

Zhaoping Lü is a vice editor-in-chief and Yuan Wu is an editorial board member for this journal. They were both not involved in the editorial review or the decision to publish this article. The authors declare that they have no known competing financial interests or personal relationships that could have appeared to influence the work reported in this paper.

References

[1] Y. Zhang, T.T. Zuo, Z. Tang, *et al*., Microstructures and properties of high-entropy alloys, *Prog. Mater. Sci.*, 61(2014), p. 1.

[2] J.J. Yi, F.Y. Cao, M.Q. Xu, L. Yang, L. Wang, and L. Zeng, Phase, microstructure and compressive properties of refractory high-entropy alloys CrHfNbTaTi and CrHfMoTaTi, *Int. J. Miner. Metall. Mater.*, 29(2022), No. 6, p. 1231.

[3] J. Wu, H.G. Zhu, and Z.H. Xie, Strength and ductility synergy of Nb-alloyed $Ni_{0.6}CoFe_{1.4}$ alloys, *Int. J. Miner. Metall. Mater.*, 30(2023), No. 4, p. 707.
[4] N. Xiao, X. Guan, D. Wang, *et al*., Impact of W alloying on microstructure, mechanical property and corrosion resistance of face-centered cubic high entropy alloys: A review, *Int. J. Miner. Metall. Mater.*, 30(2023), No. 9, p. 1667.
[5] Z.P. Lu, Z.F. Lei, H.L. Huang, *et al*., Deformation behavior and toughening of high-entropy alloys, *Acta Metall. Sin.*, 54(2018), No. 11, p. 1553.
[6] Y.F. Ye, Q. Wang, J. Lu, C.T. Liu, and Y. Yang, High-entropy alloy: Challenges and prospects, *Mater. Today*, 19(2016), No. 6, p. 349.
[7] D. Saha, E.D. Bøjesen, A.H. Mamakhel, M. Bremholm, and B.B. Iversen, *In situ* PDF study of the nucleation and growth of intermetallic PtPb nanocrystals, *Chemnanomat*, 3(2017), No. 7, p. 472.
[8] S. Maiti and W. Steurer, Structural-disorder and its effect on mechanical properties in single-phase TaNbHfZr high-entropy alloy, *Acta Mater.*, 106(2016), p. 87.
[9] L.J. Santodonato, Y. Zhang, M. Feygenson, C.M. Parish, M.C. Gao, R.K. Weber, J.C. Neuefeind, Z. Tang, and P.K. Liaw, Deviation from high-entropy configurations in the atomic distributions of a multi-principal-element alloy, *Nat. Commun.*, 6(2015), art. No. 5964.
[10] D. Han, X.J. Guan, Y. Yan, F. Shi, and X.W. Li, Anomalous recovery of work hardening rate in Cu–Mn alloys with high stacking fault energies under uniaxial compression, *Mater. Sci. Eng. A*, 743(2019), p. 745.
[11] N. Clément, D. Caillard, and J.L. Martin, Heterogeneous deformation of concentrated NiCr F.C.C. alloys: Macroscopic and microscopic behaviour, *Acta Metall.*, 32(1984), No. 6, p. 961.
[12] X.F. Chen, Z.C. Wang, and X.Y. Zhong, Developments of energy-filtered transmission electron microscopy, *J. Chin. Electron Microsc. Soc.*, 37(2018), No. 5, p. 540.
[13] A. Tamm, A. Aabloo, M. Klintenberg, M. Stocks, and A. Caro, Atomic-scale properties of Ni-based FCC ternary, and quaternary alloys, *Acta Mater.*, 99(2015), p. 307.
[14] R.P. Zhang, S.T. Zhao, C. Ophus, *et al*., Direct imaging of short-range order and its impact on deformation in Ti–6Al, *Sci. Adv.*, 5(2019), No. 12, art. No. eaax2799.
[15] Z.F. Lei, X.J. Liu, Y. Wu, *et al*., Enhanced strength and ductility in a high-entropy alloy via ordered oxygen complexes, *Nature*, 563(2018), p. 546.
[16] E. Antillon, C. Woodward, S.I. Rao, B. Akdim, and T.A. Parthasarathy, Chemical short range order strengthening in a model FCC high entropy alloy, *Acta Mater.*, 190(2020), p. 29.
[17] Q.J. Li, H. Sheng, and E. Ma, Strengthening in multi-principal element alloys with local-chemical-order roughened dislocation pathways, *Nat. Commun.*, 10(2019), No. 1, art. No. 3563.
[18] W. Guo, W. Dmowski, J.Y. Noh, P. Rack, P.K. Liaw, and T. Egami, Local atomic structure of a high-entropy alloy: An X-ray and neutron scattering study, *Metall. Mater. Trans. A*, 44(2013), No. 5, p. 1994.
[19] M.Y. Jiao, Z.F. Lei, Y. Wu, *et al*., Manipulating the ordered oxygen complexes to achieve high strength and ductility in medium-entropy alloys, *Nat. Commun.*, 14(2023), No. 1, art. No. 806.
[20] I. Lazić and E.G.T. Bosch, Chapter three–Analytical review of direct stem imaging techniques for thin samples, [in] P.W. Hawkes, ed., *Advances in Imaging and Electron Physics*, Volume 199, 2017, p. 75.
[21] I. Lazic, E.G. Bosch, S. Lazar, M. Wirix, and E. Yücelen, Integrated differential phase contrast (iDPC)–Direct phase imaging in STEM for thin samples, *Microsc. Microanal.*, 22(2016), No. S3, p. 36.
[22] E. Yücelen, I. Lazić, and E.G.T. Bosch, Phase contrast scanning transmission electron microscopy imaging of light and heavy atoms at the limit of contrast and resolution, *Sci. Rep.*, 8(2018), No. 1, art. No. 2676.
[23] Y. Zhang, W.B. Wang, W.D. Xing, *et al*., Effect of oxygen interstitial ordering on multiple order parameters in rare earth ferrite, *Phys. Rev. Lett.*, 123(2019), No. 24, art. No. 247601.
[24] Q.Q. Ding, Y. Zhang, X. Chen, *et al*., Tuning element distribution, structure and properties by composition in high-entropy alloys, *Nature*, 574(2019), p. 223.
[25] S. Dasari, A. Sharma, C. Jiang, *et al*. Srinivasan, and R. Banerjee, Exceptional enhancement of mechanical properties in high-entropy alloys via thermodynamically guided local chemical ordering, *Proc. Natl. Acad. Sci. U.S.A.*, 120(2023), No. 23, art. No. e2211787120.
[26] L. Wang, J. Ding, S.S. Chen, *et al*., Tailoring planar slip to achieve pure metal-like ductility in body-centred-cubic multi-principal element alloys, *Nat. Mater.*, 22(2023), No. 8, p. 950.
[27] X.F. Chen, Q. Wang, Z.Y. Cheng, *et al*., Direct observation of chemical short-range order in a medium-entropy alloy, *Nature*, 592(2021), No. 7856, p. 712.
[28] H.Z. Sha, J.Z. Cui, and R. Yu, Deep sub-angstrom resolution imaging by electron ptychography with misorientation correction, *Sci. Adv.*, 8(2022), No. 19, art. No. eabn2275.
[29] Z. Chen, Y. Jiang, Y.T. Shao, *et al*., Electron ptychography achieves atomic-resolution limits set by lattice vibrations, *Science*, 372(2021), No. 6544, p. 826.
[30] C. Liu, J.Z. Cui, Z.Y. Cheng, *et al*., Direct observation of oxygen atoms taking tetrahedral interstitial sites in medium-entropy body-centered-cubic solutions, *Adv. Mater.*, 35(2023), No. 13, art. No. e2209941.
[31] S. Moniri, Y. Yang, J. Ding, *et al*., Three-dimensional atomic structure and local chemical order of medium- and high-entropy nanoalloys, *Nature*, 624(2023), No. 7992, p. 564.
[32] Y. Yang, J.H. Zhou, F. Zhu, *et al*., Determining the three-dimensional atomic structure of an amorphous solid, *Nature*, 592(2021), No. 7852, p. 60.
[33] S. Tang, T.Z. Xin, W.Q. Xu, *et al*., Precipitation strengthening in an ultralight magnesium alloy, *Nat. Commun.*, 10(2019), No. 1, art. No. 1003.
[34] Z.P. Xiong, I. Timokhina, and E. Pereloma, Clustering, nano-scale precipitation and strengthening of steels, *Prog. Mater. Sci*, 118(2021), art. No. 100764.
[35] X.L. Zhou, Z.Q. Feng, L.L. Zhu, *et al*., High-pressure strengthening in ultrafine-grained metals, *Nature*, 579(2020), No. 7797, p. 67.
[36] J.P. Buban, K. Matsunaga, J. Chen, *et al*., Grain boundary strengthening in alumina by rare earth impurities, *Science*, 311(2006), No. 5758, p. 212.
[37] H.Y. Lin, P. Hua, K. Huang, Q. Li, and Q.P. Sun, Grain boundary and dislocation strengthening of nanocrystalline NiTi for stable elastocaloric cooling, *Scripta Mater.*, 226(2023), art. No. 115227.
[38] Z.D. Pan, K. Wu, X.D. Zhao, Y. Lin, and W.K. Zhang, Development of ultra high strength non-oriented silicon steel by dislocation strengthening, *Iron Steel*, 58(2023), No. 3, p. 111.
[39] M.S. Lucas, G.B. Wilks, L. Mauger, *et al*., Absence of long-range chemical ordering in equimolar FeCoCrNi, *Appl. Phys. Lett.*, 100(2012), No. 25, art. No. 251907.
[40] J.W. Yeh, S.Y. Chang, Y. der Hong, S.K. Chen, and S.J. Lin, Anomalous decrease in X-ray diffraction intensities of Cu–Ni–Al–Co–Cr–Fe–Si alloy systems with multi-principal elements, *Mater. Chem. Phys.*, 103(2007), No. 1, p. 41.
[41] S.T. Zhao, Z.Z. Li, C.Y. Zhu, *et al*., Amorphization in extreme deformation of the CrMnFeCoNi high-entropy alloy, *Sci. Adv.*, 7(2021), No. 5, art. No. eabb3108.
[42] T. Xiong, W.F. Yang, S.J. Zheng, *et al*., Faceted Kurdjumov-Sachs interface-induced slip continuity in the eutectic high-en-

tropy alloy, $AlCoCrFeNi_{2.1}$, *J. Mater. Sci. Technol.*, 65(2021), p. 216.
[43] Z.J. Zhang, M.M. Mao, J.W. Wang, *et al*., Nanoscale origins of the damage tolerance of the high-entropy alloy CrMnFeCoNi, *Nat. Commun.*, 6(2015), art. No. 10143.
[44] S.F. Liu, Y. Wu, H.T. Wang, *et al*., Stacking fault energy of face-centered-cubic high entropy alloys, *Intermetallics*, 93(2018), p. 269.
[45] Y. Deng, C.C. Tasan, K.G. Pradeep, H. Springer, A. Kostka, and D. Raabe, Design of a twinning-induced plasticity high entropy alloy, *Acta Mater.*, 94(2015), p. 124.
[46] K. Jiang, Q. Zhang, J.G. Li, *et al*., Abnormal hardening and amorphization in an FCC high entropy alloy under extreme uniaxial tension, *Int. J. Plast*, 159(2022), art. No. 103463.
[47] G. Laplanche, A. Kostka, C. Reinhart, J. Hunfeld, G. Eggeler, and E.P. George, Reasons for the superior mechanical properties of medium-entropy CrCoNi compared to high-entropy CrMnFeCoNi, *Acta Mater.*, 128(2017), p. 292.
[48] H. Wang, D.K. Chen, X.H. An, *et al*., Deformation-induced crystalline-to-amorphous phase transformation in a CrMnFeCoNi high-entropy alloy, *Sci. Adv.*, 7(2021), No. 14, art. No. eabe3105.
[49] R.M. Niu, X.H. An, L.L. Li, Z.F. Zhang, Y.W. Mai, and X.Z. Liao, Mechanical properties and deformation behaviours of submicron-sized Cu–Al single crystals, *Acta Mater.*, 223(2022), art. No. 117460.
[50] J.Q. Ding, J.D. Zuo, Y.Q. Wang, *et al*., Progress in the local chemical short-range order of multi-principal alloys, *Rare Met. Mater. Eng.*, 52(2023), No. 4, p. 1507.
[51] L.T.W. Smith, Y.Q. Su, S.Z. Xu, A. Hunter, and I.J. Beyerlein, The effect of local chemical ordering on Frank-Read source activation in a refractory multi-principal element alloy, *Int. J. Plast.*, 134(2020), art. No. 102850.
[52] Y.K. Zhao, J.M. Park, J.I. Jang, and U. Ramamurty, Bimodality of incipient plastic strength in face-centered cubic high-entropy alloys, *Acta Mater.*, 202(2021), p. 124.
[53] D. Han, Z.Y. Wang, Y. Yan, F. Shi, and X.W. Li, A good strength-ductility match in Cu–Mn alloys with high stacking fault energies: Determinant effect of short range ordering, *Scripta Mater.*, 133(2017), p. 59.
[54] Y.J. Zhang, D. Han, and X.W. Li, A unique two-stage strength-ductility match in low solid-solution hardening Ni–Cr alloys: Decisive role of short range ordering, *Scripta Mater.*, 178(2020), p. 269.
[55] Y.Q. Bu, Y. Wu, Z.F. Lei, *et al*., Local chemical fluctuation mediated ductility in body-centered-cubic high-entropy alloys, *Mater. Today*, 46(2021), p. 28.
[56] V. Gerold and H.P. Karnthaler, On the origin of planar slip in f.c.c. alloys, *Acta Metall.*, 37(1989), No. 8, p. 2177.
[57] S.I. Rao, C. Varvenne, C. Woodward, *et al*., Atomistic simulations of dislocations in a model BCC multicomponent concentrated solid solution alloy, *Acta Mater.*, 125(2017), p. 311.
[58] Z.F. He, Y.X. Guo, L.F. Sun, *et al*., Interstitial-driven local chemical order enables ultrastrong face-centered cubic multicomponent alloys, *Acta Mater.*, 243(2023), art. No. 118495.
[59] F. Zhang, Y. Wu, H.B. Lou, *et al*. Polymorphism in a high-entropy alloy, *Nat. Commun.*, 8(2017), art. No. 15687.
[60] J. Ding, Q. Yu, M. Asta, and R.O. Ritchie, Tunable stacking fault energies by tailoring local chemical order in CrCoNi medium-entropy alloys, *Proc. Natl. Acad. Sci. U.S.A.*, 115(2018), No. 36, p. 8919.
[61] R.P. Zhang, S.T. Zhao, J. Ding, *et al*., Short-range order and its impact on the CrCoNi medium-entropy alloy, *Nature*, 581(2020), No. 7808, p. 283.
[62] Z.C. Xie, W.R. Jian, S.Z. Xu, *et al*., Phase transition in medium entropy alloy CoCrNi under quasi-isentropic compression, *Int. J. Plast.*, 157(2022), No. 1, art. No. 103389.
[63] F. Walsh, M.W. Zhang, R.O. Ritchie, A.M. Minor, and M. Asta, Extra electron reflections in concentrated alloys do not necessitate short-range order, *Nat. Mater.*, 22(2023), No. 8, p. 926.
[64] E. Frely, B. Beuneu, A. Barbu, and G. Jaskierowicz, Short and long-range ordering of $(Ni_{0.67}Cr_{0.33})_{1-x}Fe_x$ alloys under electron irradiation, *MRS Online Proc. Lib.*, 439(1996), No. 1, p. 373.
[65] V.V. Sagaradze, I.I. Kositsyna, V.L. Arbuzov, V.A. Shabashov, and Y.I. Filippov, Phase transformations in Fe–Cr alloys upon thermal aging and electron irradiation, *Phys. Met. Metall.*, 92(2001), No. 5, p. 508.
[66] S. Banerjee, *In-situ* studies on phase transformations under electron irradiation in a high voltage electron microscope, *Sadhana*, 28(2003), No. 3, p. 799.